Peptides 31 (2010) 1165–1176

Contents lists available at ScienceDirect

Peptides

journal homepage: www.elsevier.com/locate/peptides

# Arachin derived peptides as selective angiotensin I-converting enzyme (ACE) inhibitors: Structure–activity relationship

V.K. Jimsheena, Lalitha R. Gowda*

*Department of Protein Chemistry and Technology, Central Food Technological Research Institute, Council of Scientific and Industrial Research, Mysore 570020, India*

ARTICLE INFO

*Article history:*
Received 12 January 2010
Received in revised form 25 February 2010
Accepted 25 February 2010
Available online 7 March 2010

*Keywords:*
Bioactive peptides
Hypertension
Tripeptide inhibitors
Molecular docking
Protease-P
*Arachis hypogaea*

ABSTRACT

Current attention focuses on mechanisms of controlling blood pressure through the inhibition of angiotensin I-converting enzyme (ACE). Bioactive antihypertensive peptides of food origin are increasingly gaining importance as alternates to synthetic drugs in hypertension therapy. The ACE inhibitory property of an enzymatic digest of arachin, the major storage globulin of peanut (*Arachis hypogaea*) has been demonstrated. The ACE inhibitory activity of a tripeptide (IEY) isolated from these digests has been characterized. Five synthetic structural analogs of this peptide (IEW, IKY, IKW, IEP and IKP) were assembled and their ACE inhibitory activity evaluated. Among these, the tripeptide IKP was a potent competitive inhibitor with an $IC_{50}$ of $7 \pm 1 \times 10^{-6}$ M similar to that of the potent whey peptides IPP and VPP. The inhibition data of these peptide analogs have been rationalized through docking simulations using the tACE–lisinopril complex at 2 Å resolution (PDB: 1086). The best docking poses were located at the tACE catalytic site resembling the mode of inhibition exerted by lisinopril, the synthetic drug. The degree of inhibition by the peptides correlated with the coordination distance between the catalytic Zn(II) and the carbonyl oxygen of the peptide bond between the amino-terminal and middle residue. These studies illustrate that these peptides, like lisinopril, behave as transition state analog inhibitors and are useful in therapeutic intervention for blood pressure management.



## 1. Introduction

Hypertension is a major public health problem, the prevalence of which is increasing alarmingly in developing as well as developed countries. Being stealthy in the progress of the disease, it can cause blood vessel changes in the retina, abnormal thickening of the heart muscle, stroke, heart attack, and arterial aneurysm, and it is a leading cause of chronic renal failure. Even a moderate elevation of arterial blood pressure leads to shortened life expectancy [14]. Renin–angiotensin system (RAS) plays a vital role in controlling hypertension. Angiotensin converting enzyme (ACE; peptidyl dipeptide hydrolase, EC 3.4.15.1), a type I membrane anchored dipeptidyl carboxypeptidase, by virtue of its ability to convert angiotensin I to a potent vasoconstrictor angiotensin II and by abolishing the vasodilator effects of bradykinin by degradation, operates as a key enzyme in the RAS [37]. A plethora of potent inhibitors have been discovered or synthesized that mainly differ from one another in potency, route of elimination, duration of action, being either prodrugs or active drugs. Synthetic ACE inhibitors, captopril (2*S*)-1-[(2*S*)-2-methyl-3-sulfanylpropanoyl] pyrrolidine-2-carboxylic acid), lisinopril (N2-[(1*S*)-1-carboxy-3-phenylpropyl]-L-lysyl-L-proline) and enalapril ((2*S*)-1-[(2*S*)-2-[(2*S*)-1-ethoxy-1-oxo-4-phenylbutan-2-yl]aminopropanoyl]pyrrolidine-2-carboxylic acid), which are developed based on snake venom peptide scaffold, have established themselves in the therapy of hypertension, congestive heart failure and diabetic neuropathy [6]. Albeit their established effectiveness, the inherently associated adverse side effects such as skin rashes, dry cough and angio-edema necessitate the need to find more natural and safer alternatives [35].

Peptides and proteins play a physiological role beyond being sources of metabolic energy and essential amino acids. The specific sequences of bioactive peptides hidden or latent in a food protein sequence can be released during proteolysis, in food processing or by gastrointestinal digestion and thereby provide physiological benefits after release. Varied bioactivities in a plethora of hydrolyzed proteins introduce a completely new dimension to be considered while enumerating and describing dietary protein quality [36]. These peptides containing only a few amino acids (di or tri peptides) will be able to cross the digestive epithelial barrier and enter the blood stream, which allows them to reach peripheral organs and exert effects. Bioactive peptides are increasingly becoming important as starting points for drugs and drug related compounds. Among the various bioactive peptides, the

* Corresponding author. Tel.: +91 821 2515331; fax: +91 821 2517233.
*E-mail addresses:* lrg@cftri.res.in, lrgowda@yahoo.com (L.R. Gowda).

0196-9781/$ – see front matter © 2010 Elsevier Inc. All rights reserved.
doi:10.1016/j.peptides.2010.02.022

antihypertensive peptides have been studied extensively. A plethora of antihypertensive peptides from enzymatic hydrolyzates of various sources like milk [5], fish [17], fermented milk [12], mushroom [16], soy bean [25,51], insect protein [47], peanut flour [34] and egg [24] have been demonstrated to inhibit ACE both in vivo and in vitro. Although there is vast information on the production and characterization of antihypertensive peptides, the information on in vitro structure–activity relationship is sparse. Peptide Quantitative Structure–Activity Relationship (QSAR) modeling has been used for predicting peptide structures with high ACE inhibitory activity. Using physicochemical descriptors, Pripp et al. [33] emphasized that increased side chain hydrophobicity at the carboxy-terminus and decreased side chain length of the penultimate amino acid exemplified ACE inhibitory potential of peptides up to six amino acids in length. ACE inhibitors reported are diverse and derived from a varied array of plant and animal origin proteins by different enzymes and hydrolysis times, advocate that a variety of peptides with various amino acid sequences are able to inhibit ACE [46]. This study was undertaken to optimize and illustrate a more systematic understanding of the relationship between the peptide structure and ACE inhibitory potential. The fact that storage proteins of oil seed meals are repositories of bioactive peptides, yet underutilized led us to carry out this study on the storage proteins of peanut (*Arachis hypogaea*).

The major proteins of peanuts are the storage globulins, arachin and conarachin I and II, and comprise nearly 75–80% of the total proteins [32]. These proteins are easily extractable in aqueous solvents. The low lysine to arginine ratio in these proteins has long been recognized as having an anti atherogenic effect [10]. The sequence of these storage proteins are intrinsically laden with bioactive peptides that need to be harnessed.

In the present investigation, the ACE inhibitory property of a Protease-P hydrolyzate of arachin, the major storage protein of peanut has been demonstrated. The hydrolyzate was further fractionated and the major ACE inhibitory tripeptide segregated from a suite of peptides and characterized. Synthetic analogs of this peptide were used to understand the structural features that contribute to ACE inhibition potency. Their interaction with the active site of human tACE was evaluated by molecular docking to comprehend the structure and specific conformations adopted by the peptide in the microenvironment to explain the differences observed in the degree of ACE inhibition.

## 2. Materials and methods

### 2.1. Materials

Peanut (*A. hypogaea*) variety TMV-2 was obtained from University of Agricultural Sciences, Gandhi Krishi Vignana Kendra (GKVK) Bangalore, India. Porcine lung and kidney acetone powders were prepared in the laboratory. Protease-P-Amano-P was from Amano Pharmaceuticals, Nagoya, Japan. Hippuryl-histidyl-leucine (HHL), hippuric acid (HA), sodium tetraborate, Triton X-100, coomassie brilliant blue G-250 (CBB G-250), coomassie brilliant blue R-250 (CBB G-250), *O*-(benzotriazol-1-yl)-*N*,*N*,*N*′,*N*′-tetramethyluronium hexa fluorophosphate (HBTU), triethylamine, ethanedithiol (EDT) and trifluoroacetic acid (TFA) were obtained from Sigma–Aldrich Chemicals Co., St. Louis, MO, USA. Fmoc (9-fluorinylmethyloxycarbonyl) protected amino acids and resins were from Novabiochem, Merck KGaA, Darmstadt, Germany and Chem Impex International, Inc., USA. Methanol (HPLC grade), acetonitrile (HPLC grade), diisopropyl ethyl amine (DIEA), dimethyl formamide (DMF), dichloromethane (DCM), thioanisole, 1-hydroxybenzotriazole (HOBT), diethyl ether, pyridine and benzene sulfonyl chloride (BSC) were from Spectrochem Pvt. Ltd., India. Amino acid standards (Pierce H.) and phenylisothiocynate (PITC) were from Pierce Chemical Company, Rockford, Illinois, USA. All other reagents and chemicals used were of analytical grade.

### 2.2. Preparation of porcine kidney and lung ACE

ACE was extracted from porcine lung and kidney acetone powder prepared in the laboratory. One gram of acetone powder was extracted with 10 mL of 0.05 M sodium borate buffer pH 8.2 containing 0.3 M NaCl and 0.5% Triton X-100 at 4 °C for 16–18 h. The extract was centrifuged at 14,100 × *g* for 60 min at 4 °C. The supernatant was dialyzed against the same buffer without Triton X-100 (1 L × 3) for 24 h and stored at −20 °C until used. The specific activities were 0.003 and 0.002 units/mg for porcine lung and kidney ACE, respectively.

### 2.3. Protein estimation

Protein concentration was determined by the method of Bradford [3]. Bovine serum albumin was used as the standard.

### 2.4. In vitro colorimetric assay for ACE

ACE activity was assayed by monitoring the release of HA from the substrate HHL as described [18]. The assay mixture contained 0.125 mL of 0.05 M sodium borate buffer pH 8.2 containing 0.3 M NaCl, 0.05 mL of 5 mM HHL and 0.025 mL of ACE enzyme extract. The reaction was arrested after incubation at 37 °C for 30 min by the addition of 0.2 mL of 1 M HCl. After stopping the reaction, 0.4 mL of pyridine was added followed by 0.2 mL of BSC and mixed by inversion for 1 min and cooled on ice. The yellow color developed was measured at 410 nm in a spectrophotometer (Shimadzu UV 1601). One unit of ACE activity is defined as the amount of enzyme, which releases 1 μmol of HA per min at 37 °C and pH 8.2.

### 2.5. In vitro assay of ACE inhibitor activity

Porcine lung or kidney ACE was preincubated (10 min) with different concentrations of the peptide fractions and the residual activity determined as described above. The $IC_{50}$ value is defined as the concentration of the peptide required to decrease the ACE activity by 50%. The percent inhibition curves were plotted using a minimum of five independent determinations for each inhibitor concentration and $IC_{50}$ values computed from the semi logarithmic plots. A linear regression analysis was performed using Origin 4.1 to evaluate the mode of inhibition and to determine the dissociation constant ($K_i$). Various concentrations of HHL were incubated with a fixed concentration of either porcine lung ACE in the presence or absence of ACE inhibitor peptides at 37 °C. The HA released was determined by the colorimetric method. The initial reaction velocities were calculated from the HA released. The type of inhibition was evaluated from Lineweaver–Burke plot [21] and the $K_i$ was calculated from a Dixon plot of the same data [9].

### 2.6. HPLC assay for the determination of ACE activity

The ACE activity was also verified by reverse phase high performance liquid chromatography (RP-HPLC) assay reported [50]. The product HA was separated from HHL by RP-HPLC on a Waters Symmetryshield octadecyl column (150 mm × 4.6 mm (i.d.), 5 μM) by isocratic elution with 50% methanol containing 0.1% TFA at a flow rate of 0.8 mL/min and detected at 228 nm.

### 2.7. Isolation of arachin

Arachin was isolated as described earlier [44]. A 10% (w/v) slurry of defatted peanut flour in 10% NaCl (w/v) was extracted by agitation for 4–6 h at 25 ± 2 °C. The extract was clarified by centrifugation 4300 × *g* for 45 min at 25 ± 2 °C. Arachin was precipitated by the addition of solid $(NH_4)_2SO_4$ to a final concentration of 40% (w/v). The precipitate obtained after centrifugation (6700 × *g*, 25 ± 2 °C, 30 min) was redissolved in 10% NaCl. The $(NH_4)_2SO_4$ precipitation was repeated three times to obtain pure arachin. The precipitated arachin dissolved in water was dialyzed extensively (1 L × 4) against distilled water, freeze dried and stored at 4 °C until further use. The purity of protein was confirmed by SDS-PAGE, amino-terminal sequencing by Edman degradation and amino acid analysis.

### 2.8. SDS-PAGE

SDS-PAGE (12.5% T, 2.7% C) was performed according to the method of Laemmli [20]. The gel was stained for protein with 0.1% coomassie brilliant blue R-250. The molecular mass of the arachin subunits were calculated using a calibration curve of log molecular weight versus relative mobility of standard molecular weight markers.

### 2.9. Preparation of arachin derived ACE inhibitor peptides

One gram of isolated arachin was suspended in 5 mL of 0.1 M Tris–HCl buffer pH 8.2 and digested with Protease-P (Amano-P from *Aspergillus niger* (2200 U/mg of protein) using an enzyme substrate ratio of 0.5%, 1.0%, 2%, 4%, 6%, 8% and 10% (w/w) at 37 °C for 4 h. The pH of the reaction mixture was maintained at 8.2 by the addition of HCl. The reaction was terminated by the addition of 100% TCA to a final concentration of 10% and cooled on ice. The hydrolyzate was centrifuged at 14,100 × *g* for 30 min at 4 °C to remove undigested protein. The supernatant containing a suite of peptides was used as the source of ACE inhibitor peptides. This suite of peptides was fractionated by RP-HPLC on a semi-preparative C-5 Phenomenex column (25 cm × 21.2 mm (i.d.), 10 μM) using a binary gradient of 0.1% TFA and 70% acetonitrile in water containing 0.05% TFA at a flow rate of 10 mL/min traversing from 0% to 100% B in 60 min. The peptides were detected at 230 nm. The peptides were further purified on the same reverse phase column using an ion pairing gradient of (A) 50 mM ammonium acetate and (B) 50 mM ammonium acetate/acetonitrile (50:50). The peptide fraction showing highest ACE inhibition was subjected to RP-HPLC on a C18 column (4.6 mm × 150 mm (i.d.), 5 μM) using TFA/acetonitrile solvent as described previously.

### 2.10. Sequence determination of the peptides by Edman degradation

The amino-terminal sequence was determined by Edman degradation using an automated Applied Biosystems 477-A gas phase sequencer equipped with an online detection system for PTH-amino acids. β-Lactoglobulin was used as standard to validate the performance of the system.

### 2.11. Amino acid analysis

The purified peptides were hydrolyzed in vacuum at 110 °C in 6 N HCl for 24 h. Amino acid analysis was performed by pre-column derivatization with PITC. The phenylthiocarbomoyl amino acids were hydrolyzed by RP-HPLC [2].

### 2.12. Fmoc solid phase peptides synthesis (Fmoc SPPS)

The acid forms of the tripeptides were assembled on an automatic peptide synthesizer (Model CS 136, CS Bio Co. San Carlos, CA, USA) using standard Fmoc chemistry. Fmoc-L-Trp-2-chlorotrityl and Fmoc-L-Pro-2-chlorotrityl resins preloaded with the first amino acid were used for peptides containing carboxy-terminal Trp and Pro respectively. Fmoc-Tyr (tBu)-Wang resin was used for peptides containing carboxy-terminal Tyr.

The sequence of the tripeptides was verified by amino-terminal sequencing and amino acid analysis. Semi-preparative HPLC was carried out using Shimadzu HPLC equipped with a LC8A pump on a C-18 Shimpak column (25 cm × 21.2 mm (i.d.), 10 μM) and a binary gradient of 0.1% TFA and 70% acetonitrile in water containing 0.05% TFA at a flow rate of 15 mL/min traversing from 0% to 100% B in 60 min. Data were collected via a SPD-M10AVP photodiode array detector at 230 nm. Purity of all the peptides was >99% as determined by RP-HPLC.

### 2.13. In vitro stability of the peptides

In vitro stability against gastric proteases was assessed by incubating a 0.1% (w/v) peptide solution in 0.01 N HCl with pepsin for 2 h at 37 °C, the reaction was stopped by boiling in a water bath for 10 min and neutralized, and residual ACE inhibitor activity determined. Stability was similarly assessed using pancreatin in 0.02 M Tris–HCl, pH 8.2 at 37 °C for 2 h.

### 2.14. Molecular docking

The model for ACE used in this study was derived from the coordinates of the structure labeled 1086 in the Brookhaven Protein Data Bank, which represents the human tACE bound to lisinopril at 2 Å resolution [28]. The structure of the tripeptides was constructed and optimized using the polypeptide builder function of the public domain web server PepBuild which uses SCRWL to predict the conformations of the side chains and optimizes using rotameric libraries (www.imtech.res.in/bvs/pepbuild/method.html) [41]. Explicit hydrogens in the peptide structures were assigned using PepBuild and saved in the MOL format. The possibility of binding, precise location of binding sites and mode of binding for each ligand was carried out independently using an automated docking software, Molgro Virtual Docker 2008, version 3.2.1 (Molgro ApS, Aarhus, Denmark, http://molegro.com), that is based on guided differential evolution and a force field based screening function [43]. Possible binding conformations and orientations were analyzed by clustering methods, embedded in MolDock.

All docking studies were carried out using the crystal structure of tACE complexed with the inhibitor lisinopril (PDB: 1086) as the template. All water molecules and the inhibitor lisinopril were excluded, whereas zinc and chloride atoms were retained in the active site, fixed to their crystal positions, throughout the docking process. The molecular structures of the imported ligands were manually checked before docking and corrected. The initial geometry and topologies of the protein and the ligands were retrieved to the docking software Molgro Virtual Docker. The binding site was computed within a spacing of *x*: 37.26, *y*: 35.35 and *z*: 46.21 such that the binding site of tACE was well sampled with a grid resolution of 0.3 Å. Each ligand (peptides) was then individually docked into this grid using the MolDock Optimizer algorithm, and its interactions monitored using detailed energy estimates. Clustering was performed based on the similarities in binding modes and strengths in these cycles and ignoring similar poses. A value of population size and maximum interactions 100 and 10,000 respectively were used for each run and 5 best poses were retained for each lig-

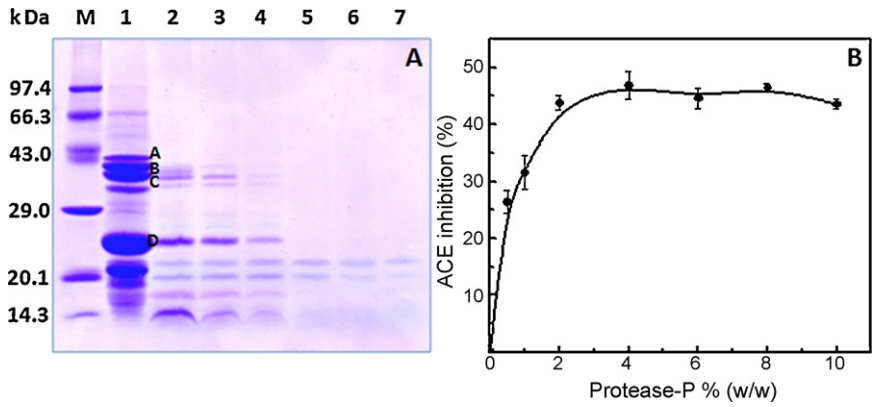


**Fig. 1.** (A) SDS-PAGE profile (12.5% T, 2.7% C) of Protease-P hydrolyzates of arachin. Lane M. Molecular weight markers (phosphorylase b ($M_r$ 97,400 Da); bovine serum albumin ($M_r$ 66,300 Da); ovalbumin ($M_r$ 43,000 Da), carbonic anhydrase ($M_r$ 29,000 Da), soybean trypsin inhibitor ($M_r$ 20,100 Da), lysozyme ($M_r$ 14,300 Da), lane 1: arachin (control), lanes 2–7: arachin digested using enzyme to arachin ratio of 0.5, 1, 2, 4, 6 and 8%, respectively. ~75 μg of protein loaded per well. B. The effect of enzyme/arachin ratio on ACE inhibitory activity of the digests. ACE inhibition was assayed using the colorimetric method.

and. Lisinopril was docked into the template structure as a positive control and the RMSD obtained. The docking mode obtained from this validation exercise superposed well with that of the crystal structure given credence by the minimal RMSD of 0.4 Å obtained. Predicted low binder tripeptide, AVP [31] was used as negative control. The software Discovery Studio Visualizer 2.5.1 (Accelrys Software Inc., http://www.accelrys.com) was utilized to establish hydrogen bonds and hydrophobic interactions between residues at the ACE active site and the peptide poses.

### 2.15. Data analysis

For all the measurements, a minimum of 3–5 replicates was taken for data analysis. Using the software Origin 4.1, all of the values were averaged and mean values are reported. The standard deviation of 5 different replicate data was also tabulated.

## 3. Results

### 3.1. Isolation of arachin

Arachin, the major storage globulin of peanut was isolated to apparent homogeneity. The subunit architecture was evaluated by SDS-PAGE (Fig. 1A). The results show that it is contains 12 subunits as reported earlier [1]. The amino acid composition (data not shown), amino-terminal sequence and estimated molecular mass of the subunits (Fig. 1A and Table 1) correspond to that reported for arachin in the Protein Data Bank. The subunits A, B and C (Fig. 1A) based on their molecular mass and amino-terminal sequence (Table 1) can be classified as the acidic subunits. The release of glycine as the amino-terminal of the subunit D and its mass renders it as a basic subunit. These results indicate the purified arachin is homogenous and can be used for further analyses.

### 3.2. ACE inhibition of arachin fungal protease digests

The arachin extracted from peanut meal was digested with different concentrations of Protease-P (Amano-P from *A. niger* (2200 U/mg of protein). The extent of digestion was analyzed by SDS-PAGE (Fig. 1A). The results indicate that maximum digestion was accomplished with 2% (w/w) of enzyme. A further increase in the enzyme substrate ratio had appeared to have no effect on the digestion pattern (Fig. 1A, lanes 3–6). The acidic subunits (A–C) of molecular mass 35,500–40,500 Da were extremely susceptible to proteolysis. Similarly the basic subunit (Fig. 1A) was degraded completely. The digestion with different enzyme substrate ratios results in the release of peptides of ≈14,300–20,000 Da that is resistant to further digestion. The ACE inhibitory potential of the crude proteolytic digests was evaluated against porcine lung ACE. The results indicate that maximum inhibition (47 ± 2%) was achieved at an enzyme substrate ratio of 4% (w/w). Increasing the enzyme concentration thereafter did not enhance the ACE inhibitory activity (Fig. 1B). These results are in concurrence with changes observed in the peptide profile on increasing enzyme concentration (Fig. 1A). The ACE inhibitory potential of the digests towards lung and kidney was similar. The suite of peptides following Protease-P digestion (4%, w/w) was selected for further characterization.

### 3.3. Isolation of ACE inhibitor peptide

Semi-preparative RP-HPLC of the Protease-P hydrolyzate on a C-5 column resulted in three major peptide fractions with a considerable number of minor peptides (Fig. 2). Among the major peptide fractions, fraction 1 (retention time = 30.74 min) exhibited the highest ACE inhibitor activity (Fig. 2 inset). This peptide fraction was subsequently fractionated by ion-pair chromatography using an ammonium acetate/acetonitrile solvent system. This peptide fraction was further re-chromatographed on the same column using the TFA/$CH_3CN$ solvent system. The RP-HPLC profile showed a sin-

**Table 1**
The amino-terminal sequences of arachin subunits.

| Subunit no.[a] | Amino-terminal sequence | $M_r$ (kDa) | PDB accession no. |
|---|---|---|---|
| A | ISFYQQPEENACQQQYLNAQQ. . . | 42 ± 1 | ACH91862 |
| B | ISFYQHPEENAAQFQYLNA. . . | 38 ± 1 | ABL14270 |
| C | VTFRQGGEENECQFQRLNA. . . | 35 ± 1 | ABI17154 |
| D | GIEEGIRGASVKSNDGYNEQADIYXPQ. . . | 24 ± 1 | AAW56067 |

[a] The subunit numbers as labeled in Fig. 1A. Following SDS-PAGE the protein bands were transferred to a PVDF membrane in 0.01 M CAPS-10% methanol buffer (pH 11) and stained with coomassie brilliant blue R-250. The bands were excised, washed with methanol and loaded directly to the Applied Biosystems 477A automated gas phase sequencer for N-terminal sequencing by Edman degradation.

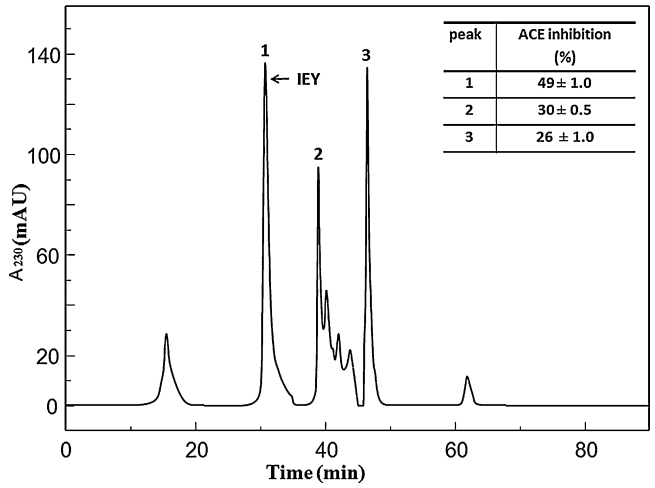


**Fig. 2.** RP-HPLC profile of Protease-P digest of arachin at an enzyme/arachin ratio of 4% (w/w). The peptides were resolved on a semi-preparative C5 column (25 cm × 21.2 mm (i.d.), 10 μM) using a gradient of acetonitrile and water containing 0.05% TFA. Inset: ACE inhibitory activity of peptide fractions, assayed by the colorimetric method using porcine lung ACE and HHL as the substrate.

gle peak indicating the peptide was homogeneous. The purified peptide inhibited both porcine lung and kidney ACE.

### 3.4. Characterization of the ACE inhibitor peptide

The amino acid composition of the purified peptide was determined after hydrolysis in vacuo with 6 M HCl at 110 °C for 24 h. The amino acid composition indicated the presence of only 3 amino acids, Ile, Glu and Tyr in equimolar concentration. The amino acid sequence of the peptide was found to be Ile–Glu–Tyr (IEY) and theoretical molecular weight of the peptide was ≈423 Da. The sequence IEY corresponded to the sequence $Ile^5$–$Tyr^7$ of the 21,000 Da sub unit of arachin (PDB: P20780).

The tripeptide IEY was assembled by solid phase peptide synthesis using Wang resin and Fmoc chemistry and purified by RP-HPLC. The homogeneity of the peptide was validated by the single peak observed with a retention time of 18.97 min (Fig. 3A). The purity was >99%. The peptide sequence was verified by Edman degradation. The inhibitory potential of the synthetic peptide towards porcine lung ACE was evaluated. The synthetic peptide was an inhibitor of porcine lung ACE with an $IC_{50}$ of 182 ± 2 μM (Table 2 and Fig. 4A). The effect of the tripeptide on varying substrate concentrations plotted as a Lineweaver–Burk plot (data not shown) indicated that the synthetic peptide was a competitive inhibitor with respect to the substrate HHL. The equilibrium dissociation constant $K_i$ calculated from the Dixon plot of the data shown in Fig. 4B was 83.53 μM (Fig. 4C). The $IC_{50}$ value of IEY is several fold higher than that reported for the antihypertensive tripeptides VPP (9 μM) and IPP (5 μM) derived from milk protein [31].

**Table 2**
Inhibition of porcine lung ACE activity by the tripeptides calculated as $IC_{50}$ (μM).

| Peptide | $IC_{50}$ (μM) |
|---|---|
| IEY | 182 ± 4 |
| IEW | 104 ± 3 |
| IEP | 18 ± 2 |
| IKY | 34 ± 3 |
| IKW | 19 ± 2 |
| IKP | 7 ± 1 |
| IEP + IEY | 132 ± 5 |
| IEP + IEW | 101 ± 4 |
| IEY + IEW | 107 ± 4 |
| IEP + IEY + IEW | 146 ± 3 |

The values are an average of five replicates. The $IC_{50}$ values were determined using the colorimetric assay and validated using the HPLC method.

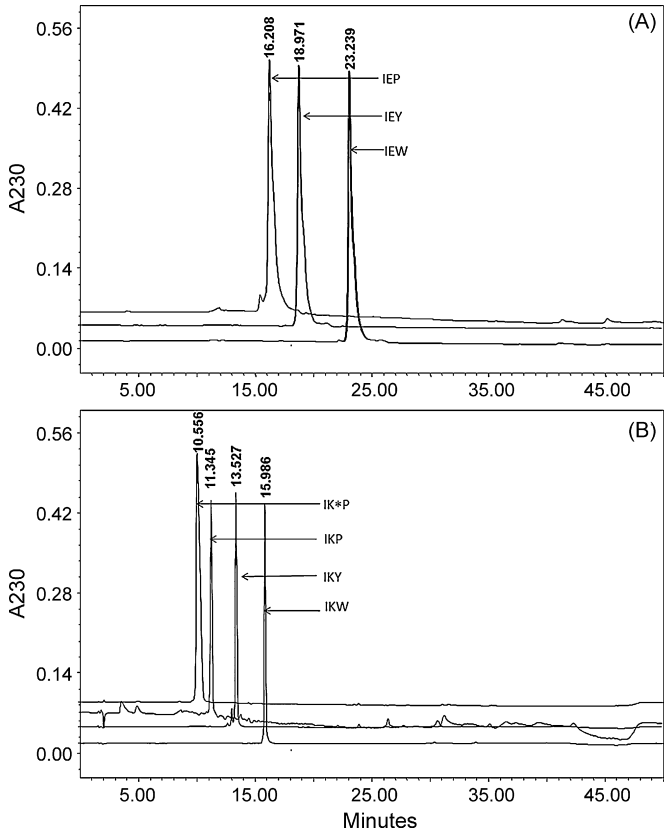


**Fig. 3.** RP-HPLC profile indicating the homogeneity of the peptides synthesized by Fmoc chemistry. The purity of the peptides was analyzed using a C18 column (150 mm × 4.6 mm (i.d.), 5 μM) on a Waters Associate HPLC, with a gradient of 0.1% TFA and 70% acetonitrile containing 0.05% TFA. (A) IEP, IEY and IEW. (B) IKP, IKY, IKW and IK*P.

### 3.5. Peptide analogs of IEY and ACE inhibition

Previous structure–activity relationship studies predict that a tripeptide with a bulky aliphatic residue at the amino-terminal such as Leu/Ile, a positively charged residue at the middle position and an aromatic residue or Pro at the carboxy-terminus will emerge as potent ACE inhibitor peptides [49]. The characterized peptide IEY satisfies these criteria with the exception that the middle position holds a negatively charged acidic amino acid. Could this difference be responsible for the elevated $IC_{50}$ of IEY? To answer this question, tripeptide analogs of IEY using various amino acid substitutions at the middle and carboxy-terminal positions were synthesized and the $IC_{50}$ values for the inhibition of porcine lung ACE determined. Initially, the carboxy-terminal Tyr was replaced with a bulkier aromatic residue Trp (W) or Pro (P). For a second replacement, the negatively charged middle amino acid Glu (E) was exchanged for a positively charged Lys (K). Consequently, the following peptides IEW, IEP, IKY, IKW and IKP were synthesized. These tripeptides were assembled by standard Fmoc chemistry using Fmoc protected amino acids as building blocks and were purified by preparative RP-HPLC. The single peaks obtained by analytical RP-HPLC thereafter suggest that the peptides were pure and homogenous (Fig. 3A and B). The purity of all the peptides was >99%. The sequences of the synthetic peptides were further validated by Edman degradation and amino acid analyses.

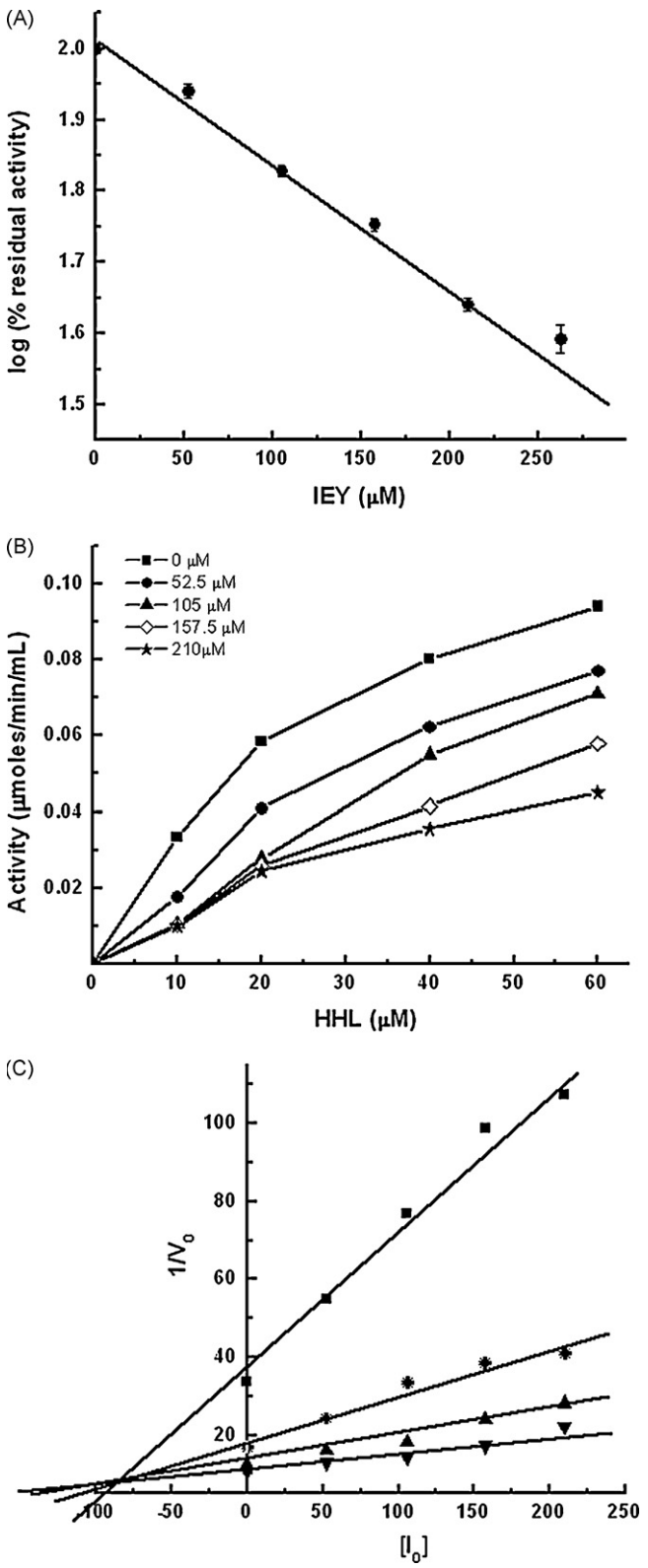


**Fig. 4.** Kinetic analysis of the tripeptide IEY/porcine lung ACE complexation consistent with a reversible and competitive inhibition. ACE activity was determined as described under methods either in the absence or presence of the indicated tripeptide concentrations. (A) The semi logarithmic plot to determine $IC_{50}$ of IEY, (B) Michaelis–Menten curve showing the inhibition in presence of different concentration of IEY and (C) Dixon plot of the data in part B used to determine $K_i$ (the data represent means of triplicate experiments with SEM never exceeding 4%).

Porcine lung ACE was preincubated for 10 min with varying concentrations of each of these peptides. The residual ACE activity was determined as described. Semi logarithmic plots were used to determine $IC_{50}$ values (Table 2). The results suggest that substituting Pro for Tyr at the carboxy-terminal of the tripeptide increased the potency 10-fold whereas the bulkier Trp did not significantly enhance inhibition ($IC_{50}$ 182–104 μM). Replacing the acidic Glu with Lys increased the inhibitory potential by 5-fold. The synergistic effect of these two changes was evident from the much lower $IC_{50}$ of IKP which was 17-fold more potent than the isolated peptide IEY. The $IC_{50}$ of $7 \pm 1$ μM of IKP is similar to that reported for potent antihypertensive peptides IPP and VPP derived from milk proteins. The observation that the parent crude digest, which contains a suite of peptides, always exhibits a much higher inhibition than the peptides in isolation led us to evaluate synergism if any, between the peptides. The results (Table 2) however suggested that there was no apparent increase in inhibitory potency among these peptides used in combination. These results coupled with the competitive inhibition observed for the individual peptides are suggestive of a single binding site on ACE. Kinetic analysis of the most potent tripeptide IKP-porcine lung ACE complexation was consistent with a reversible and competitive mechanism of inhibition (results not shown) with respect to the substrate HHL. The binding affinity ($K_i$) of IKP to ACE was $2.7 \times 10^{-6}$ M as calculated from the Dixon plot.

### 3.6. *In vitro stability of the peptides to gastrointestinal digestion*

ACE inhibitor peptides for therapeutic use must be resistant to gastrointestinal proteolysis once they are ingested orally in order to reach the target tissue and exert an antihypertensive effect. The stability of each of the purified peptide was assessed in vitro in order to predict their antihypertensive potential in vivo. The inhibitory potential of all the peptides were preserved after digestion with pepsin. However, the tripeptides IKY and IKP were partially stable to the consecutive digestion with pancreatin (contains trypsin and chymotrypsin) (Table 3). This decrease in ACE inhibition can be attributed to the hydrolysis by trypsin at the carboxyl-end of Lys of the peptides. Among the synthetic peptides, IKP was the most potent inhibitor of porcine lung ACE, yet it was more susceptible to in vitro digestion with pancreatin (Table 3). Therefore to increase the in vitro stability and to decrease the susceptibility to pancreatin digestion, the tripeptide IK*P was synthesized replacing L-Lys with

**Table 3**
In vitro stability of the peptides to gastrointestinal proteases[a].

| Peptide | Protease | ACE inhibition (%) |
|---|---|---|
| IEP | Control | 100 |
| | Pepsin | 99 |
| | Pancreatin | 100 |
| IEY | Control | 100 |
| | Pepsin | 99 |
| | Pancreatin | 100 |
| IEW | Control | 100 |
| | Pepsin | 100 |
| | Pancreatin | 100 |
| IKP | Control | 100 |
| | Pepsin | 100 |
| | Pancreatin | 66 |
| IKY | Control | 100 |
| | Pepsin | 99 |
| | Pancreatin | 75 |
| IKW | Control | 100 |
| | Pepsin | 100 |
| | Pancreatin | 97 |

[a] The ACE inhibition is the mean of three experiments. The SEM was ≤3% in each case.

**Table 4**
Experimental binding constants, predicted binding energies and Zn(II) coordination distances of tripeptide with tACE (PDB: 1086).

| Ligand | $K_i$ (μM) | Affinity energy (kJ/mol, pose) | Zn(II) coordination | |
|---|---|---|---|---|
| | | | Distance (Å) | Atom |
| Lisinopril | 0.001 | | 2.141 | Carboxyl group of lisinopril |
| IKP | 2.66 | −13.45 (00) | 2.730 | Carbonyl oxygen of the peptide bond between I and K |
| IEP | 7.24 | −15.43 (02) | 3.036 | Carbonyl oxygen of the peptide bond between I and E |
| IKW | 8.5 | −18.20 (00) | 3.299 | Carbonyl oxygen of the peptide bond between I and K |
| IKY | 12.96 | −15.80 (00) | 3.445 | Carbonyl oxygen of the peptide bond between I and K |
| IEW | 55.01 | −17.50 (01) | – | No Zn(II) coordination |
| IEY | 83.53 | −15.57 (00) | – | No Zn(II) coordination |

D-Lys. The peptide albeit resistant to proteolysis by pancreatin did not inhibit either porcine lung or kidney ACE at concentrations as high as 5 mM. These results indicate that the stereo-specificity of the amino acid residue plays a vital role in ACE inhibition.

### 3.7. Molecular docking

Automated docking simulations were performed with tACE and the tripeptide inhibitors to correlate the amino acid substitutions in the tripeptides with the changes in the ACE inhibitor potential observed. Human sACE is composed of two homologous domains (N and C-domain) having ≈60% sequence identity, each one with a functional catalytic site that comprises the highly conserved HEXXH Zinc binding motif [7,8,45], with C-domain being the dominant angiotensin converting site [28]. As the sequence of tACE and C-domain of sACE are identical; all the docking studies were carried out with tACE.

A molecular docking algorithm Molegro Dock based on a heuristic search algorithm that uses a cavity prediction algorithm [43] was used to elucidate the mode of interactions between the tACE and the tripeptide ACE inhibitors. To evaluate the effectiveness of the MolDock programme in the docking of the inhibitor tripeptides, we first docked lisinopril and compared the resulting geometry with the corresponding crystal structure of tACE-lisinopril complex (PDB: 1086). The best returned pose in presence of Zn(II) with a docking score of 154.43 (Table 4), revealed the same ACE residues involved in Zn(II) coordination. The main interactions considered responsible for the high potency of this drug have been reproduced by this docking procedure (Tables 4–6). These include (1) carboxy alkyl carboxylate and Zn(II) coordination and the H-bond with $Glu^{384}$ (OE2 atom) and (2) the H-bond between the carboxy-terminal carboxylate of lisinopril interaction with $Lys^{511}$ and $Tyr^{520}$ at the S1′ subsite. These results validate the docking accuracy for further studies with the inhibitor tripeptides.

The best poses of the docking study of the tripeptides at tACE catalytic site in presence of Zn(II) are shown in Fig. 5. The best poses for each of these tripeptides was stabilized by H-bonds and hydrophobic interactions with tACE residues (Tables 5 and 6). The molecular docking of the tripeptides on the binding site of tACE reveal that these peptides are buried deep inside the active site channel similar to lisinopril in the tACE-lisinopril complex [28]. The molecular docking studies revealed that these six bioactive peptides occupy mainly the S2′ subsite and are also accommodated in the hydrophobic pocket with hydrophobic interactions with $Phe^{512}$, $Phe^{527}$, $Phe^{457}$or $Val^{518}$. The carbonyl oxygen of the peptide bond between the P1 and P1′ residues (Schechter and

**Table 5**
Residues of tACE having at least one atom at a distance of 3.5 Å around the docked peptide. The residues around crystallized lisinopril in the tACE (PDB: 1086) are also shown. The residue numbers areas of tACE (PDB: 1086).

| No. | tACE residues | Lisinopril | IEY | IEW | IEP | IKY | IKW | IKP |
|---|---|---|---|---|---|---|---|---|
| 1. | ALA354 | √ | √ | √ | √ | √ | √ | √ |
| 2. | ALA356 | | √ | √ | | √ | | √ |
| 3. | ARG522 | | | | | √ | | |
| 4. | ASP377 | | √ | | | | √ | |
| 5. | ASP415 | | | √ | | | | |
| 6. | CYS352 | | √ | | | | √ | √ |
| 7. | GLN281 | √ | | √ | √ | √ | √ | √ |
| 8. | GLU162 | √ | √ | | | √ | √ | √ |
| 9. | GLU376 | | | | | | √ | |
| 10. | GLU384 | √ | √ | √ | √ | √ | √ | √ |
| 11. | GLU411 | √ | √ | √ | √ | | | |
| 12. | HIS353 | √ | √ | √ | √ | √ | √ | √ |
| 13. | HIS383 | √ | √ | √ | √ | √ | | √ |
| 14. | HIS387 | √ | √ | √ | | √ | | √ |
| 15. | HIS513 | √ | √ | √ | √ | √ | √ | √ |
| 16. | LYS368 | | | √ | | | | |
| 17. | LYS511 | √ | | √ | | √ | √ | √ |
| 18. | PHE457 | | | √ | √ | | | √ |
| 19. | PHE512 | | | √ | √ | | √ | √ |
| 20. | PHE527 | | | √ | √ | | | |
| 21. | SER355 | | √ | √ | √ | √ | √ | √ |
| 22. | TRP357 | | | √ | | | | |
| 23. | TYR520 | √ | | √ | √ | √ | √ | √ |
| 24. | TYR523 | √ | √ | √ | √ | √ | √ | √ |
| 25. | VAL380 | | √ | | | √ | √ | √ |
| 26. | VAL518 | | √ | | √ | | | |
| 27. | GLN369 | | √ | | | | | |
| Total | | 12 | 16 | 19 | 14 | 15 | 15 | 17 |

(√) indicates the presence of the residue.

Berger nomenclature) [38] of all the peptides except IEY and IEW are positioned to coordinate the active site Zn(II) atom (Fig. 5). This coordination coupled with that of $His^{383}$, $His^{387}$of the α13 helix and $Glu^{411}$ affords a tetrahedral geometry in semblance to the distorted tetrahedral geometry of lisinopril/captopril-tACE complex. The direct coordination with the catalytic Zn(II) and the carbonyl oxygen of the peptide bond between Ile and Lys in the IKP is almost the same order reported for captopril (2.32 Å). It is conceivable that the distance between the peptide bond carbonyl oxygen and Zn(II) account for the varied degrees of inhibition by these peptides. Shorter the Zn(II) distance to the carbonyl oxygen of the peptide, the greater the degree of inhibition (Table 4). This Zn(II) coordina-

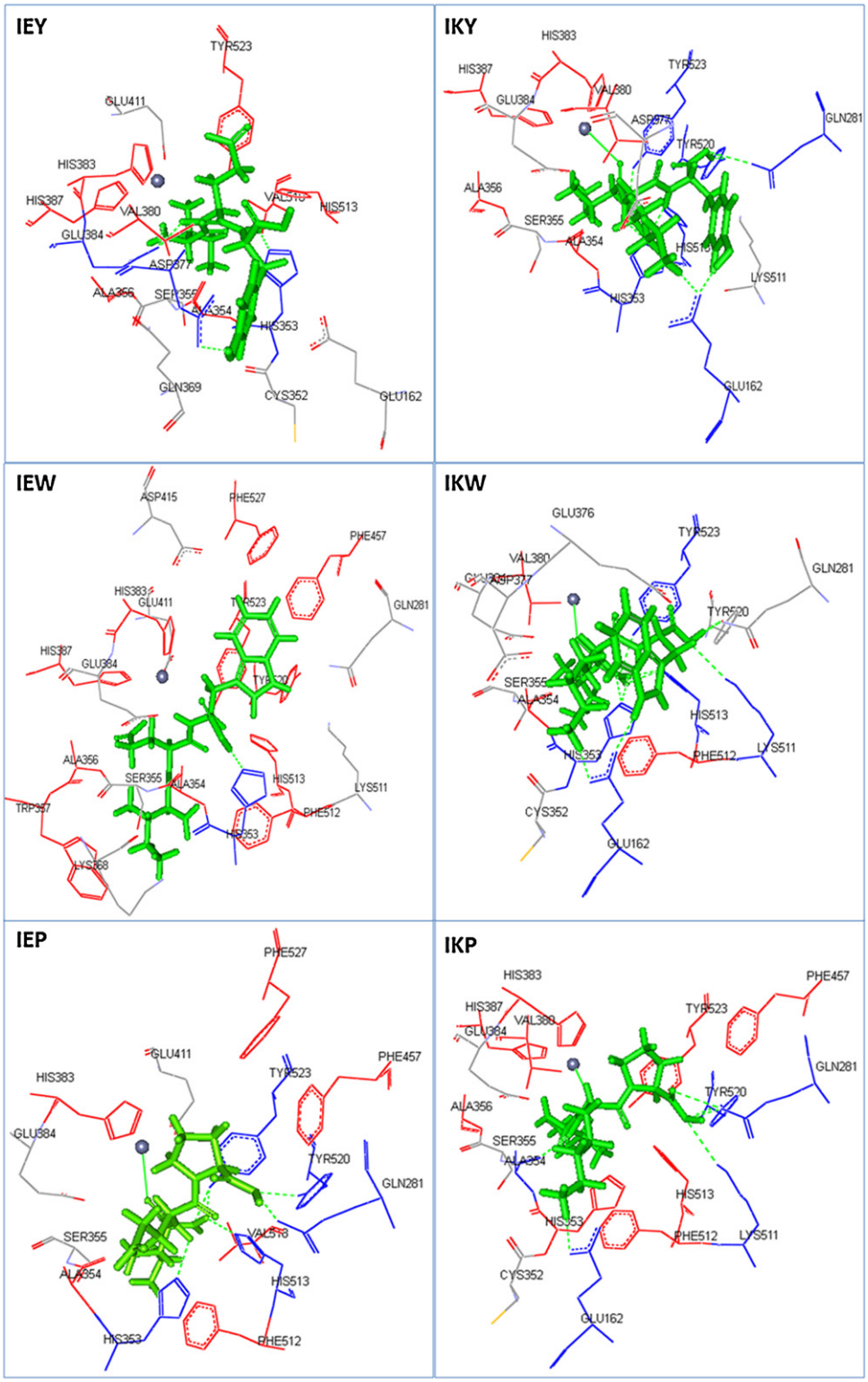


**Fig. 5.** Predicted binding mode of peptide inhibitors to tACE (PDB: 1086). The best ranked docking pose is shown. Stereo image of catalytic binding site of tACE. Lisinopril from the PDB structure was eliminated and peptides docked at the active site. Peptide ligands are shown in stick model. Zn(II) is shown as a circle. Dotted lines indicate hydrogen bonds and bold line indicates Zn(II) coordination with the peptide backbone.

**Table 6**
Hydrogen bonds observed between the docked top ranked pose of peptides and tACE. The residue numbers are as of tACE (PDB: 1086).

| tACE residues in H-bonding | Number of H-bonds and their corresponding distance (Å) | | | | | | |
|---|---|---|---|---|---|---|---|
| | Lisinopril[a] | IEY | IKP | IEW | IEP | IKY | IKW |
| ALA354:O | 1 (2.9) | – | 1 (2.2) | – | – | – | – |
| GLN281:NE2 | – | – | 2 (2.9, 2.9) | – | 1 (2.6) | 1 (3.2) | – |
| GLU162:OE1 | – | – | 1 (1.9) | – | – | 2 (1.6, 1.7) | 1 (1.9) |
| GLU162:OE2 | 1 (3.4) | – | – | – | – | – | 1 (1.9) |
| HIS353:NE2 | 1 (2.8) | 1 (2.2) | – | 1 (1.8) | 1 (2.4) | 3 (2.3, 1.9,2.4) | 2 (2.1, 1.7) |
| HIS513:NE2 | 1 (3.1) | – | – | – | 1 (2.2) | 1 (2.3) | 2 (2.4, 2.4) |
| LYS511:NZ | 1 (2.9) | – | 1 (3.1) | – | – | – | 1 (3.0) |
| TYR520:OH | 1 (2.6) | – | 1 (2.8) | – | 1 (2.6) | 2 (2.6, 1.6) | 2 (2.71.6) |
| TYR523:OH | 1 (2.8) | – | – | – | 2 (2.6, 1.8) | 1 (2.9) | 1 (3.0) |
| GLU384:OE2 | 1 (2.7) | 2 (2.3, 2.2) | – | – | – | – | – |
| ASP377:OD2 | – | 1 (1.9) | – | – | – | – | – |
| Total | 8 | 4 | 6 | 1 | 6 | 10 | 10 |

–: H-bond not observed.
[a] H-bonds observed in the crystallized tACE-lisinopril complex (PDB: 1086).

tion distance for IKP is 2.73 Å and IKP is 3-fold more potent than IEP for which the coordinating distance is 3.036 Å (Table 4).

The results show that bulky aromatic residues at the carboxy-terminus (P2′) result in the carbonyl oxygen of the P1–P1′ bond being rotated such that it does not coordinate to Zn(II) (Fig. 5, IEY and IEW) thus explaining the higher $IC_{50}$ values (Table 2). The replacement with a Lys (positive charge) for the Glu (negative charge) leads to a weak Zn(II) coordination and a concomitant increase in the ACE inhibition (Table 2). These results are in accordance with the prediction that a positively charged amino acid residue adjacent to an aromatic residue is essential for ACE inhibitor activity [19].

The H-bonding interactions between the carboxy-terminal carboxylate of lisinopril and $Tyr^{520}$ and $Lys^{511}$ of tACE provide a solitary and significant mode of inhibitor registration strategy like the substrate substance-P [26]. The functional importance of this carboxy-terminal carboxylate docking interaction in ACE inhibition is revealed by comparing IEY and IEW with the other tripeptides. The absence of H-bond interaction of IEY and IEW with both $Tyr^{520}$ and $Lys^{511}$ of tACE (Fig. 5 and Table 6) are commensurate with the elevated $IC_{50}$ values. It is possible that by virtue of steric hindrance, the aromatic residues of IEY and IEW prevent the H-bond formation between the carboxy-terminal carboxylate and $Lys^{511}$. Substituting Glu with Lys restores a hydrogen bond interaction between the carboxy-terminal carboxylate of IKW with $Lys^{511}$ and $Tyr^{520}$ (Table 6). This also explains why IKW ($IC_{50} = 19 \pm 2\ \mu M$) exhibits a better ACE inhibition than IKY ($IC_{50} = 34 \pm 3\ \mu M$), in addition to the Zn(II) coordinating distances. The tripeptide IEP although lacking a H-bond to $Lys^{511}$ of tACE, a strong interaction observed with $Tyr^{520}$ is probably a significant part of the inhibitor registration strategy. The most potent porcine lung ACE inhibitor among the tripeptides is IKP (Table 2). IKP not only registers both the crucial H-bond interactions with tACE ($Lys^{511}$ and $Tyr^{520}$) necessary for carboxylate docking but also reveals an interaction with $Glu^{162}$ (OE1) and $Ala^{354}$ (O). The lysyl amine forms a very strong hydrogen bond with Glu 162 (OE1 atom, 1.9 Å) at the S1′ subsite of tACE probably responsible for the tight binding ($2.7 \times 10^{-6}$ M). The weak H-bond between $Glu^{162}$ (OE2, 3.4) observed with lisinopril is absent with IKP similar to that observed for captopril and enalapril and the bioactive whey peptides IPP and VPP [31]. The positioning of H-bond from $Tyr^{523}$ present in lisinopril-tACE complex is lost in the IKP-tACE model. In contrast, the H-bond to the carboxyl group of Ala 354 (O) between P1 and P1′ is much stronger (2.2 Å). The two H-bonds from $His^{513}$ and $His^{353}$ are also lost. The amino-terminal Ile interacts with $Phe^{512}$ and $Val^{518}$ of the hydrophobic pocket. The lisinopril-tACE and IKP-tACE complexes superimposed (Fig. 6) suggest a similar inhibition mechanism.

These findings highlight the importance of both carboxylate docking and carboxy-terminal residue side chain interactions and the coordination distance to the carboxyl oxygen in between P1 and P1′ site, in defining peptide ACE inhibitor potency.

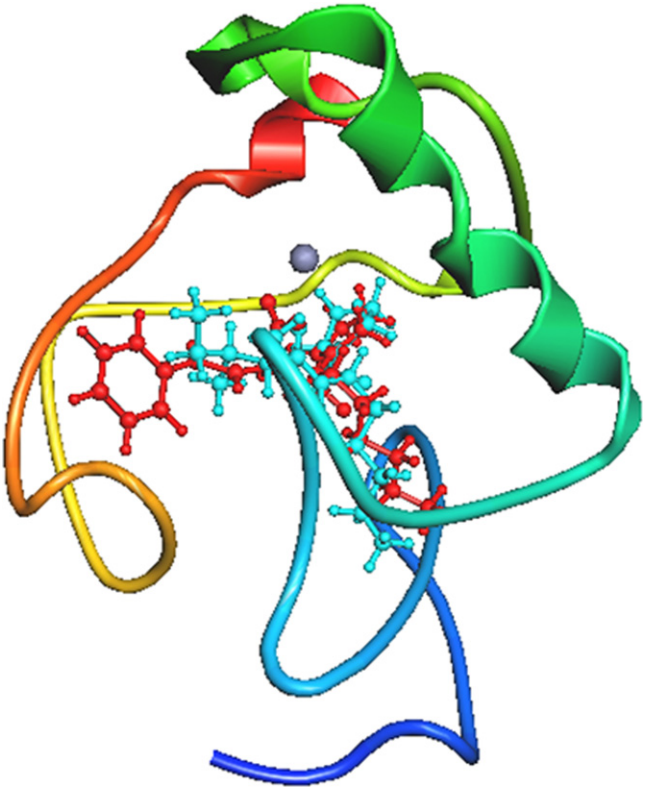

**Fig. 6.** The ball and stick models of IKP (cyan) and lisinopril (red) superimposed at the active site of tACE (PDB: 1086). (For interpretation of the references to color in this figure legend, the reader is referred to the web version of the article.)

## 4. Discussion

Natural components in foods with prophylactic and therapeutic benefits include bioactive peptides that exhibit antihypertensive properties. ACE inhibitor peptides, as a part of food product or as a nutraceutical, especially when derived from a food protein of plant or animal origin, are of functional interest as they would have no harmful side effects [15]. A very large cache of food derived antihypertensive peptides have been categorized based on their origin: animal derived, plant derived and microorganisms [15]. Despite

this vast array of bioactive peptides as an alternate line of therapy to control mild hypertension, the exact mode and mechanism of ACE inhibition is not clearly understood other than reported in vitro and in vivo studies. The available crystal structures of human sACE and tACE [8,26–28] with deep insights to the specificity and physiological significance of the active site are a platform for understanding the mode of inhibition of food derived peptides.

The health promoting properties of peanut protein have been well documented. Arachin and conarachin, the major storage globulins of peanut account for nearly 75% of the total protein [32]. Arachin and its molecular species, separated and identified by amino-terminal analyses (Fig. 1A), were similar to that reported earlier [1,39–40]. The high arginine to lysine ratio of arachin coupled with the putative antihypertensive peptide sequences encrypted in the available protein sequence data for arachin subunits was the premise to prepare enzymatic hydrolyzate and study their antihypertensive potential. Accordingly, the proteolysis of arachin was engineered and Protease-P hydrolyzate contained a suite of potent ACE inhibitory peptides. The SDS-PAGE profile shows the disintegration of the arachin larger subunits on hydrolysis, leaving no visible bands of the high molecular weight bands (Fig. 1A). It could therefore be said that it is the small peptide units that are responsible for ACE inhibition. Both the acidic and basic subunits of arachin were vulnerable to digestion, similar to that observed for roasted peanuts [34]. An array of proteases viz pepsin, trypsin, chymotrypsin, pronase and actinase have been used to generate hydrolyzates that exhibit ACE inhibition. Previously Mallikarjun Gouda et al. [25] demonstrated that among several proteases used to hydrolyze glycinin, the soybean storage protein, Protease-P digests showed the highest ACE inhibition. Very recently Quist et al. [34], in an in vitro study, used pepsin–pancreatin to simulate human digestion and alcalase an industrially important enzyme to digest peanut flour. The alcalase system produced more potent antihypertensive peptides compared to the pepsin–pancreatin system.

The peptides in the enzyme digests were subsequently fractionated and purified (Fig. 2). ACE inhibitory activity could be ascribed to a tripeptide IEY. The sequence corresponded to the amino acids 5–7 of arachin segment (PDB: P20780) and in close agreement to the determined amino acid composition. This peptide is a true inhibitor and therefore useful for therapeutic intervention in blood pressure management. Previously, we isolated a penta-peptide from the enzymatic hydrolyzates of glycinin, the major storage protein of soybean [25]. Very recently, a tetrapeptide (KFAR) isolated from an alcalase treated peanut hydrolyzate showed an $IC_{50}$ of 134.4 μg/mL [13], which is much higher in comparison to the tripeptides (Table 2). Liu et al. [22] used antibodies raised against an ACE inhibitory peptide isolated from lactic acid bacteria fermentation of soybean meal extracts to detect ACE inhibitor peptides. Several other plant proteins are a source of various peptides with antihypertensive activity [15]. The chemically synthesized tripeptide (IEY) was a competitive inhibitor (Fig. 4C) with an $IC_{50}$ of $\approx 182 \pm 4$ μM. This $IC_{50}$ value is very high when compared to the ACE inhibitory peptides reported for other food proteins [15].

The ACE inhibitor peptide derived from arachin contains Ile at the amino-terminus and Tyr, at the carboxy-terminus. Cheung et al. [4] suggest that the most favored amino-terminal residues are branched chain amino acids and Pro is among the most favored carboxy-terminus residues. Pripp et al. [33] thoroughly examined ACE inhibitory peptides by QSAR methodology using physicochemical descriptors. Their results emphasized that increased side chain hydrophobicity at the carboxy-terminus and decreased side chain size of the penultimate amino acid enhanced ACE inhibitory potential for peptides containing up to six amino acids and no such relationship existed for the amino-terminal residue. Further, Wu et al. [49] modeled food based di and tripeptides from the three z-scores of amino acids and proposed ACE inhibitor peptides with higher potency than reported earlier. For tripeptides, the most preferred residue for the amino-terminus was a hydrophobic amino acid, a positively charged middle amino acid and favored an aromatic residue at the carboxy-terminus. Accordingly, the ACE inhibitory tripeptide of arachin 'IEY' fulfills these criteria with respect to the amino- and carboxy-terminus except for the middle residue Glu which is negatively charged. Given these considerations we questioned whether substituting Lys (positively charged) would enhance the ACE inhibition efficiency. The peptide IKY was assembled by chemical synthesis and the $IC_{50}$ ($34 \pm 3$ μM) for porcine lung ACE, showed it was six times more potent (Table 2). Replacing Tyr with a bulkier Trp (IKW) increased the potency two times (Table 2). Kobayashi et al. [19] showed that IKW was four times more potent than IKY against rabbit lung ACE. Therefore among the aromatic residues, the largest amino acid Trp at the carboxy-terminus showed highest ACE inhibitory activity. A substitution of Lys for Arg in tripeptide reportedly had little effect on ACE inhibition [19]. In this study, the Arg replacement was not studied. Wu et al. [49] also show that a tripeptide IKY had a log $IC_{50}$ of −0.68. Our results are in accordance with the prediction that a positively charged residue adjacent to an aromatic residue is essential for a high ACE inhibitory activity. Different ACE inhibition assays, source of ACE and calculations for the median inhibitory concentration ($IC_{50}$) hamper the comparison of ACE inhibitory activities of these tripeptides to that reported in literature.

In this study, IKP was the most potent ACE inhibitory peptide with an $IC_{50}$ value comparable to VPP and IPP (5 and 9 μM), the famous antihypertensive milk peptides [11,23]. The tripeptide IKP is also located within the glycinin G1 precursor of soybean and legumin I precursor of garden pea [49] and the observed log $IC_{50}$ was 0.44 as against the QSAR predicted 0.37. Although the most favored carboxy-terminus amino acids reported were aromatic amino acids, our study shows that Pro was superior, as IKP was three times more potent than IKW (Table 2). These results coupled with the extremely high potency of the well known milk tripeptides IPP and VPP, exemplify Pro as the favored carboxy-terminus amino acid. Among the *N*-carboxy methyl transition state peptide analogs, those with Lys-Pro at the carboxy-terminus inhibited ACE at the nanomolar levels [30]. Cheung et al. [4] also demonstrated that the inhibitory potency of dipeptides with Trp, Tyr or Pro at the carboxy-terminus were 300-fold higher than Gly. In summary, a carboxy-terminal Lys-Pro is an important facet of ACE peptide inhibitors.

The physiological antihypertensive effect of ACE inhibitory peptides is guaranteed by their bio-availability and predominantly characterized by their resistance to gastrointestinal degradation and efficient intestinal absorption [48]. In vitro simulated gastric digestion provides practical mimics of the fate of such peptides after oral administration. Although IKP showed the highest inhibitory activity, it was relatively less stable under gastrointestinal conditions compared to the other peptides of this study (Table 3). A D-amino acid substitution although increased the stability yet lost its ACE inhibitory property. The tripeptides IKP, IKW and IKY exhibit promising properties for ACE inhibition in vitro plausibly due to their small size and hydrophobic character. Small peptides can enter the peripheral blood stream intact due to their low molecular size and exert systemic effects or produce local effects in the digestive tract [53]. Further it has been suggested that ACE inhibitory peptides may exert an additional antihypertensive effect by inhibiting chymase [52].

There exists very limited information on the relationship between primary structure and ACE inhibitor potency of food protein derived antihypertensive peptides. A more profound understanding of the tripeptide inhibitor binding mode to ACE has many potentially favorable consequences. Therefore using molec-

ular docking studies, our aim was to understand the exact mode of interaction of these tripeptides with human tACE catalytic site and compare them with the manner in which captopril and lisinopril, the synthetic drugs complex with ACE and inhibit it. As a consequence of human tACE and C-domain of sACE being identical the molecular modeling was carried out using the tACE-lisinopril complex X-ray crystal structure [28]. The modeling results with tACE (Fig. 5) indicate that the tripeptides bind to ACE with high similarity to lisinopril. The best poses obtained for the tripeptides IKP, IKY, IKW and IEP show the coordination of the carbonyl group between P1 and P1′ residues, directly with the catalytic Zn(II) at the active site of tACE. Coupled with this, Zn(II) is coordinated to $His^{383}$, $His^{387}$ and $Glu^{411}$ in a distorted tetrahedral geometry, inhibiting ACE. The ACE inhibitor potency follows the order IKP > IEP > IKW > IKY > IEW > IEY. The absence of Zn(II) coordination in the tACE complex with IEW and IEY explains their very high $IC_{50}$ values. As the distance between the coordinating carbonyl oxygen of the peptide and Zn(II) increases, ACE inhibition decreases. IPP and VPP, the milk peptides coordinate to Zn(II) through the carbonyl oxygen at 2.51 and 2.66 Å respectively and IPP is the more potent ACE inhibitor [31]. Similarly IKP (2.71 Å) with the shortest coordination distance, is the most potent inhibitor among the tripeptides tested (Table 2). Interestingly, the trend of relative inhibitor potencies correlates with the coordinating distance between Zn(II) and the peptides (Table 4). A tryptophan analog at the P2′ position of lisinopril resulted in a 25–100-fold higher C-domain selectivity as compared to lisinopril [29]. The direct interaction with Zn(II) in the potent synthetic drugs is through the thiol group of captopril and the carboxyl groups of enalaprilat and lisinopril [27] and not the peptide bond, and are much shorter (2.1 Å for lisinopril), which probably explains the $IC_{50}$ in the nanomolar range. In the Drosophila homologue of ACE which has 40% sequence identity, the catalytic Zn(II) binds to the carbonyl group between P1 and P1′ site [42]. The distance between the phenyl carbonyl of the analog and the Zn(II) in the C-domain was 2.73 Å [29].

The relative inhibitor potencies of the synthetic drugs were attributed to the number of interactions in the crystal complex with tACE. No such trend was observed with the tripeptides (Table 5). IEW, which is ≈15 times less efficient than IKP shows the highest number of interactions with tACE. The observation that both IEW and IEY lack the H-bonds to $Lys^{511}$ and $Tyr^{520}$ whereas IKW and IKY form these bonds suggests that the Lys at the P1 position orients the peptide favorably for this H-bond formation with the carboxylate of the P2′ carboxy-terminus. In the structure of tACE bound to lisinopril, the terminal P2′ is stabilized by $Lys^{511}$ and $Tyr^{520}$ [42]. The best poses obtained for IKP reveal interactions with ACE via H-bonding similar to the inhibition mode of the common drug lisinopril (Fig. 6, Tables 5 and 6). In addition, the atoms coordinating the catalytic Zn(II) resemble the tetrahedral coordination geometry of lisinopril. It is conceivable that the tripeptide IKP like lisinopril is a transition state analog and inhibits ACE through a mechanism similar to that of the drug. The molecular docking studies indicate that the Zn(II) coordination distance between the P1 and P1′ carbonyls in the tripeptides is important for ACE inhibition potency. This molecular docking study has paved the way to explain the biological activities of tripeptide ACE inhibitors and provides a platform to design better peptide inhibitors.

## 5. Conclusion

Inhibiting ACE by food protein derived peptides to treat hypertension appears to be attractive because of the abrogation of adverse side effects normally accompanying synthetic drugs. A number of food peptides either derived using enzymes or through processing are known to reduce blood pressure. The concerted effort of identifying a tripeptide from enzymatic digestion of arachin, the storage protein of peanut (*A. hypogaea*) and demonstrating its ACE inhibiting capacity has led to the design and synthesis of potent tripeptide ACE inhibitors. The tripeptides have favorable competitive type inhibitory properties and are resistant to rapid biodegradation by proteases of the gastrointestinal tract. The molecular modeling technique coupled with the biological assays for ACE inhibition indicates that the tripeptides bind at the catalytic cleft of tACE with the carbonyl carbon of P1–P1′ residue coordinating Zn(II) to complete the tetrahedral geometry. The interaction of the tripeptide IKP with tACE, which has pronounced in vitro ACE inhibitory activity ($IC_{50}$ = 7 μM) is similar to lisinopril and can be considered as a transition state inhibitor and therefore find applications in therapeutic blood pressure management.

## Acknowledgements

We thank Dr. V. Prakash, Director, CFTRI, Mysore and Dr. A.G. Appu Rao, Head, PCT, CFTRI, Mysore for their advice and useful discussions. VKJ acknowledges a Senior Research Fellowship from CSIR, India. This work was carried out under CSIR-Networking Project CMM-0014 and MLP-077.

## Appendix A. Supplementary data

Supplementary data associated with this article can be found, in the online version, at doi:10.1016/j.peptides.2010.02.022.

## References

[1] Bhushan R, Agarwal R. Reversed-phase high-performance liquid chromatographic, gel electrophoretic and size exclusion chromatographic studies of subunit structure of arachin and its molecular species. Biomed Chromatogr 2006;20:561–8.
[2] Bidlingmeyer BA, Cohen SA, Tarvin TL. Rapid analysis of amino acids using precolumn derivatization. J Chromatogr 1984;336:93–104.
[3] Bradford MM. A rapid and sensitive method for the quantitation of microgram quantities of protein utilizing the principle of protein-dye binding. Anal Biochem 1976;72:248–54.
[4] Cheung HS, Wang FL, Ondetti MA, Sabo EF, Cushman DW. Binding of peptide substrates and inhibitors of angiotensin-converting enzyme. Importance of the COOH-terminal dipeptide sequence. J Biol Chem 1980;255:401–7.
[5] Clare DA, Swaisgood HE. Bioactive milk peptides: a prospectus. J Dairy Sci 2000;83:1187–95.
[6] Coppey LJ, Davidson EP, Rinehart TW, Gellett JS, Oltman CL, Lund DD, et al. ACE inhibitor or angiotensin II receptor antagonist attenuates diabetic neuropathy in streptozotocin-induced diabetic rats. Diabetes 2006;55:341–8.
[7] Corradi HR, Chitapi I, Sewell BT, Georgiadis D, Dive V, Sturrock ED, et al. The structure of testis angiotensin-converting enzyme in complex with the C domain-specific inhibitor RXPA380. Biochemistry (Mosc) 2007;46:5473–8.
[8] Corradi HR, Schwager SL, Nchinda AT, Sturrock ED, Acharya KR. Crystal structure of the N domain of human somatic angiotensin I-converting enzyme provides a structural basis for domain-specific inhibitor design. J Mol Biol 2006;357:964–74.
[9] Dixon M. The graphical determination of $K_m$ and $K_i$. Biochem J 1972;129:197–202.
[10] Erdmann K, Cheung BWY, Schröder H. The possible roles of food-derived bioactive peptides in reducing the risk of cardiovascular disease. J Nutr Biochem 2008;19:643–54.
[11] FitzGerald RJ, Meisel H. Milk protein-derived peptide inhibitors of angiotensin-I-converting enzyme. Br J Nutr 2000;84(Suppl. 1):S33–7.
[12] Gobbetti M, Ferranti P, Samacchi E, Goffredi F. Production of angiotensin-1-converting enzyme inhibitory peptides in fermented milks started by *Lactobacillus delbruekii* subsp. *bulgaricus* SS1 and *Lactococcus lactis* subsp. *cremoris* FT5. Appl Environ Microbiol 2000;66:3898–904.
[13] Guang C, Phillips RD. Plant food-derived angiotensin I converting enzyme inhibitory peptides. J Agric Food Chem 2009;57:5113–20.
[14] Guyton AC, John EH. Text book of human physiology. W.B. Saunders Co.; 2006. p. 228.
[15] Hong F, Ming L, Yi S, Zhanxia L, Yongquan W, Chi L. The antihypertensive effect of peptides: a novel alternative to drugs? Peptides 2008;29:1062–71.
[16] Hyoung Lee D, Ho Kim J, Sik Park J, Jun Choi Y, Soo Lee J. Isolation and characterization of a novel angiotensin I-converting enzyme inhibitory peptide derived from the edible mushroom *Tricholoma giganteum*. Peptides 2004;25:621–7.

[17] Ichimura T, Hu J, Aita DQ, Maruyama S. Angiotensin I-converting enzyme inhibitory activity and insulin secretion stimulative activity of fermented fish sauce. J Biosci Bioeng 2003;96:496–9.
[18] Jimsheena VK, Gowda LR. Colorimetric, high-throughput assay for screening Angiotensin I-converting enzyme inhibitors. Anal Chem 2009;81:9388–94.
[19] Kobayashi Y, Yamauchi T, Katsuda T, Yamaji H, Katoh S. Angiotensin-I converting enzyme (ACE) inhibitory mechanism of tripeptides containing aromatic residues. J Biosci Bioeng 2008;106:310–2.
[20] Laemmli UK. Cleavage of structural proteins during the assembly of the head of bacteriophage T4. Nature 1970;227:680–5.
[21] Lineweaver H, Burk D. The determination of enzyme dissociation constants. J Am Chem Soc 1934;56:658–66.
[22] Liu Li-na, Zhang Sheng-hua, He Dong-ping. Detection of an angiotensin converting enzyme inhibitory peptide from peanut protein isolate and peanut polypeptides by Western blot and dot blot hybridization. Eur Food Res Technol 2009;230:89–94.
[23] López-Fandiño R, Otte J, van Camp J. Physiological, chemical and technological aspects of milk-protein-derived peptides with antihypertensive and ACE-inhibitory activity. Int Dairy J 2006;16:1277–93.
[24] Majumder K, Wu J. Angiotensin I converting enzyme inhibitory peptides from simulated in vitro gastrointestinal digestion of cooked eggs. J Agric Food Chem 2009;57:471–7.
[25] Mallikarjun Gouda KG, Gowda LR, Rao AG, Prakash V. Angiotensin I-converting enzyme inhibitory peptide derived from glycinin, the 11S globulin of soybean (*Glycine max*). J Agric Food Chem 2006;54:4568–73.
[26] Naqvi N, Liu K, Graham RM, Husain A. Molecular basis of exopeptidase activity in the C-terminal domain of human angiotensin I-converting enzyme: insights into the origins of its exopeptidase activity. J Biol Chem 2005;280:6669–75.
[27] Natesh R, Schwager SL, Evans HR, Sturrock ED, Acharya KR. Structural details on the binding of antihypertensive drugs captopril and enalaprilat to human testicular angiotensin I-converting enzyme. Biochemistry (Mosc) 2004;43:8718–24.
[28] Natesh R, Schwager SL, Sturrock ED, Acharya KR. Crystal structure of the human angiotensin-converting enzyme–lisinopril complex. Nature 2003;421:551–4.
[29] Nchinda AT, Chibale K, Redelinghuys P, Sturrock ED. Synthesis and molecular modeling of a lisinopril-tryptophan analogue inhibitor of angiotensin I-converting enzyme. Bioorg Med Chem Lett 2006;16:4616–9.
[30] Patchett AA, Harris E, Tristram EW, Wyvratt MJ, Wu MT, Taub D, et al. A new class of angiotensin-converting enzyme inhibitors. Nature 1980;288:280–3.
[31] Pina AS, Roque AC. Studies on the molecular recognition between bioactive peptides and angiotensin-converting enzyme. J Mol Recognit 2009;22:162–8.
[32] Prakash V, Rao MSN. Physicochemical properties of oilseed proteins. CRC Crit Rev Biochem 1986;20:265–363.
[33] Pripp AH, Isaksson T, Stepaniak L, Sørhaug T. Quantitative structure–activity relationship modelling of ACE-inhibitory peptides derived from milk proteins. Eur Food Res Technol 2004;219:579–83.
[34] Quist EE, Phillips RD, Saalia FK. Angiotensin converting enzyme inhibitory activity of proteolytic digests of peanut (*Arachis hypogaea* L.) flour. LWT – Food Sci Technol 2009;42:694–9.
[35] Riordan JF. Angiotensin-I-converting enzyme and its relatives. Genome Biol 2003;4:225.
[36] Rutherfurd-Markwick KJ, Moughan PJ. Bioactive peptides derived from food. J AOAC Int 2005;88:955–66.
[37] Ryan JW, Ryan US, Schultz DR, Whitaker C, Chung A. Subcellular localization of pulmonary antiotensin-converting enzyme (kininase II). Biochem J 1975;146:497–9.
[38] Schechter I, Berger A. On the size of the active site in proteases. I. Papain. Biochem Biophys Res Commun 1967;27:157–62.
[39] Shetty KJ, Rao MS. Studies on groundnut proteins. III. Physicochemical properties of arachin prepared by different methods. Anal Biochem 1974;62: 108–20.
[40] Shetty KJ, Rao MS. Studies on groundnut proteins. V. Physico-chemical properties of arachin prepared by different methods. Anal Biochem 1976;73: 458–70.
[41] Singh B. PepBuild: a web server for building structure data of peptides/proteins. Nucleic Acids Res 2004;32:W559–61.
[42] Sturrock ED, Natesh R, van Rooyen JM, Acharya KR. Structure of angiotensin I-converting enzyme. Cell Mol Life Sci 2004;61:2677–86.
[43] Thomsen R, Christensen MH. MolDock: a new technique for high-accuracy molecular docking. J Med Chem 2006;49:3315–21.
[44] Tombs MP. An electrophoretic investigation of Groundnut proteins: the structure of arachin A and B. Biochem J 1965;96:119.
[45] Tzakos AG, Gerothanassis IP. Domain-selective ligand-binding modes and atomic level pharmacophore refinement in angiotensin I converting enzyme (ACE) inhibitors. Chem BioChem 2005;6:1089–103.
[46] van der Ven C, Gruppen H, de Bont DBA, Voragen AGJ. Optimisation of the angiotensin converting enzyme inhibition by whey protein hydrolysates using response surface methodology. Int Dairy J 2002;12:813–20.
[47] Vercruysse L, Van Camp J, Morel N, Rouge P, Herregods G, Smagghe G. Ala-Val-Phe and Val-Phe: ACE inhibitory peptides derived from insect protein with antihypertensive activity in spontaneously hypertensive rats. Peptides 2010;31:482–8.
[48] Vermeirssen V, Van Camp J, Verstraete W. Bioavailability of angiotensin I converting enzyme inhibitory peptides. Br J Nutr 2004;92:357–66.
[49] Wu J, Aluko RE, Nakai S. Structural requirements of angiotensin I-converting enzyme inhibitory peptides: quantitative structure–activity relationship study of di- and tripeptides. J Agric Food Chem 2006;54:732–8.
[50] Wu J, Ding X. Characterization of inhibition and stability of soy protein-derived angiotensin 1-converting enzyme inhibitory peptides. Food Res Int 2002;35:367–75.
[51] Wu J, Ding X. Hypotensive and physiological effect of angiotensin converting enzyme inhibitory peptides derived from soy protein on spontaneously hypertensive rats. J Agric Food Chem 2001;49:501–6.
[52] Yamamoto N, Takano T. Antihypertensive peptides derived from milk proteins. Nahrung 1999;43:159–64.
[53] Yoshikawa M, Fujita H, Matoba N, Takenaka Y, Yamamoto T, Yamauchi R, et al. Bioactive peptides derived from food proteins preventing lifestyle-related diseases. BioFactors 2000;12:143–6.